Collaborative oscillatory fracture
Supplemental Material

Juan-Francisco Fuentealba[1],* Joel Marthelot[2], Benoît Roman[3], and Francisco Melo[1,4]
[1]*Departamento de Física Universidad de Santiago de Chile, Avenida Ecuador 3493, 9170124 Estación Central, Santiago, Chile.*
[2]*Aix-Marseille Univ, CNRS, IUSTI, 13013 Marseille, France.*
[3]*PMMH, CNRS UMR 7636, UPMC, Univ. Paris 6 & Univ. Paris Diderot Paris 7, ESPCI Paris, 10 rue Vauquelin, 75231 Paris Cedex 05, France.*
[4]*SMAT-C, Universidad de Santiago, Avenida B. O'Higgins 3363, Santiago-Chile*
(Dated: March 26, 2020)

I. GENERAL PROPAGATION OF FRACTURE AND DEBONDING FRONT

We give here a quick review of several fracture situation (previously described in other works) and put them in the same framework developed in this article. These configurations serve as the basis for comparison, and were used to prepare initial conditions for 3-crack interaction in the present study.

A. Isolated channel cracks

We start by the well described isolated "channel crack" in a material under bi-axial stress. In our notations, the energy released during propagation is γeh on each side of the fracture cut (per unit increment of crack area). We recall that e is the elastic energy per unit area in the film and that γ is a non-dimensional number that depends on the relative mechanical properties of the layer and substrate. Griffith's criterion therefore reads [1]

$$2\gamma eh = G_c \tag{1}$$

where G_c is the fracture energy.

It was shown that when adhesion is decreased, fracture propagation is favored through the collaborative effect of delamination which results into two remarkable modes of regular fracture propagation, the duo and the follower modes [2, 3], that we review now.

B. Duo of cracks.

In the duo mode, two cracks are observed to propagate parallel to each other, and are joined at their tips by a straight delamination front with a very specific length l_d (Fig. S1a).

We therefore consider the general situation of two cracks delimiting an extended debonding zone. Here we take the energy difference with the pristine state as

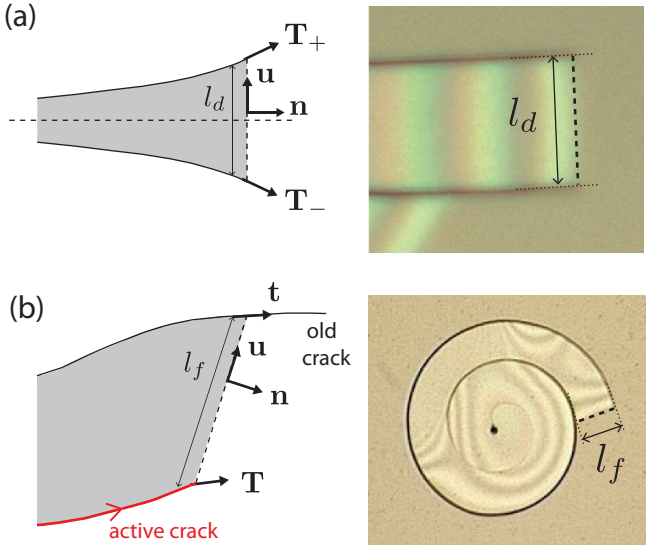

FIG. S1. a) Duo of crack. Sketch of the duo configuration (left). Snapshot of duo of cracks (right). (b) Follower crack. Sketch of a follower crack (left). Snapshot of an example of follower crack observed in a spiral crack propagation (right).

$\mathcal{E}_r = eA + ef(l) + \gamma eh(S_+ + S_-)$, where l is the length of the debonding front, and S_+ (resp S_-) the curvilinear abscissa for the position of the upper (resp inferior) fracture tip along its trajectory. Griffith's criterion for crack S_+ reads

$$d\mathcal{E}_r = \Gamma dA + G_c h dS_+,$$

where Γ is the debonding energy. Experimentally the adhesion energy is found to increase with the velocity of the delamination front (see section III for the experimental characterization of the adhesion energy) consistently with a simple linear relation:

$$\Gamma(v) = \Gamma_0 \left(1 + \frac{v}{\eta}\right) \tag{2}$$

when $\Gamma \gtrsim \Gamma_0$ where η is a kinetic parameter that has to be determined experimentally. This variation of the adhesion energy with velocity is based on experimental observations, but other generic kinetic laws are considered in section IV of Supplemental Material.

* juan.fuentealbadu@usach.cl

Denoting $\mathbf{n}$ the unit vector normal to the front, $\mathbf{u}$ its tangent vector pointing towards the crack S_+ chosen as reference, and $\mathbf{T}_+$ its direction of propagation (see the sketch in Fig. S1a), simple geometry gives $2dA = l(\mathbf{n}.\mathbf{T}_+)dS_+$ and $dl = (\mathbf{u}.\mathbf{T}_+)dS_+$ so that Griffith's criterion can be rewritten as

$$\frac{l}{2}[e-\Gamma(V_+)]\mathbf{n}.\mathbf{T}_+dS_+ + ef'(l)\mathbf{u}.\mathbf{T}_+dS_+ + \gamma ehdS_+ = G_chdS_+,$$

which we rewrite in a condensed way as

$$\mathbf{F}_+.\mathbf{T}_+ + \gamma eh = G_ch, \tag{3}$$

with the notation $\mathbf{F}_+ = [e-\Gamma(V_+)](l/2)\mathbf{n} + ef'(l)\mathbf{u}$. We recognize on the left-hand side of equation (3) the Energy Release Rate for the fracture (integrated over the thickness). We assume that fracture propagates in the direction of maximum energy release rate, so in direction $\mathbf{T}_+$ aligned along $\mathbf{F}_+$. In that case, equation (3) becomes $|\mathbf{F}_+| + \gamma eh = G_ch$ and sets the value of adhesion energy $\Gamma(V_+)$, and therefore the velocity of the crack V_+ through (2).

A similar treatment for crack S_- gives

$$\mathbf{F}_-.\mathbf{T}_- + \gamma eh = G_ch, \tag{4}$$

with the notation $\mathbf{F}_- = [e-\Gamma(v_-)]l/2\mathbf{n} - ef'(l)\mathbf{u}$. These equations provide similarly the direction of propagation $\mathbf{T}_-$ (aligned along $\mathbf{F}_-$) and the speed v_-.

We have therefore found the propagation rules for the two cracks, and it is found that in general they converge toward a "duo" state with a constant distance l_d, in which both vectors $\mathbf{T}_\pm$ are perpendicular to the debonding front (therefore along $\mathbf{n}$), which imposes that l_d obeys $f'(l_d) = 0$. Since $f(l) = \beta lh - \alpha l^2$, with α and β dimensionless constants (see main text, and [2, 3]), we finally obtain $l_d = \beta h/2\alpha$.

C. Follower crack

We observe that sometimes a fracture propagates nearly parallel to the path of a preexisting cut (as observed for example in spiral crack propagation in Fig. S1b). We call it a case of "follower crack". We note that the debonding front joins the crack, that we note S to a point with abscissa s along the pre-existing crack (see the sketch in Fig. S1b). For simplicity we consider the case of a straight pre-existing fracture, along a direction vector $\mathbf{t}$.

We now must compute the energy difference with respect to state including the pre-existing crack. The energy difference therefore is $\mathcal{E}_r = eA + ef(l) + \gamma ehS - \gamma ehs$, where $-\gamma ehs$ corresponds to the stress already released by the pre-existing crack. We use the same geometrical convention with vector $\mathbf{u}$ pointing towards the crack tip. The dynamics of the debonding front may be determined by applying Griffith's criterion, for a fixed crack position

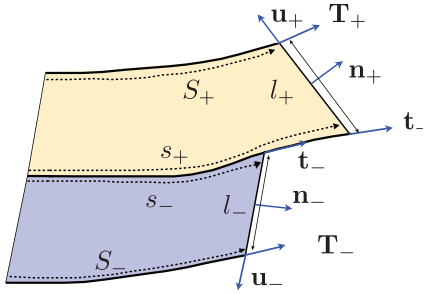

FIG. S2. Sketch of the three cracks interactions.

$d\mathcal{E}_r = d(\Gamma A)$.

$$\frac{1}{2}(e-\Gamma)l\mathbf{n}.\mathbf{t}ds - ef'(l)\mathbf{u}.\mathbf{t}ds - \gamma ehds = 0$$

(where $\mathbf{t}$ is the unit vector tangent to the pre-existing cut), which can also be written

$$\mathbf{f}.\mathbf{t} = \gamma eh \tag{5}$$

where we have noted

$$\mathbf{f} = \mathbf{n}[e-\Gamma(v)]l/2 - e(\beta h - 2\alpha l)\mathbf{u}. \tag{6}$$

This equation provides the speed $v = ds/dt$ of the point where the debonding front joins the pre-cut.

We next look for the direction and speed of the crack S using Griffith's criterion $d\mathcal{E}_r = d(\Gamma A) + G_chdS$ which leads to

$$\frac{1}{2}[e-\Gamma(V)]l\mathbf{n}.\mathbf{T}dS + ef'(l)\mathbf{u}.\mathbf{T}dS + \gamma ehds = G_chdS,$$

and we recover equation (3). The same analysis provides the direction, along vector

$$\mathbf{F} = [e-\Gamma(V)](l/2)\mathbf{n} + ef'(l)\mathbf{u} \tag{7}$$

and the speed $V = dS/dt$ of the fracture tip. Here we have discarded geometrical factors and assumed for simplicity that the velocity of the debonding front is equal to that of the crack. This approximation is fully justified when $\mathbf{t}$ and $\mathbf{n}$ vectors are nearly parallel.

This provides propagation law for both point (s, S). It is often found that the crack tends to follow geometry of the pre-cut trajectory at a distance l_f from it [2, 3]. Analytical solution in the case of a straight pre-cut is reported in [2, 3]. The delamination front makes here a defined angle with the preexisting crack and has a well defined length $l_f \sim 32h > l_d$.

D. Three cracks interactions

Here the energy difference with respect to the pristine state is

$$d\mathcal{E}_r = edA + ef'(l)dl \pm \gamma ehds \tag{8}$$

where, (+) holds for a the part in yellow in Fig. S2, while (-) holds for the part in grey. As in the main text, we choose here to consider the case where the front edge s_- lags behind the center crack s_+. The surface variations in terms of $ds_\pm$ and $dS_\pm$ (see Fig. S2) writes,

$$dA_\pm = \frac{l_\pm \mathbf{n}_\pm \cdot (\mathbf{T}_\pm dS_\pm + \mathbf{t}_\pm ds_\pm)}{2}, \tag{9}$$

and expressing $dl_\pm$ in terms of $ds_\pm$ and $dS_\pm$, we find

$$dl_+ = \mathbf{u}_+ \cdot (-\mathbf{t}_+ ds_+ + \mathbf{T}_+ dS_+) \tag{10}$$
$$dl_- = \mathbf{u}_- \cdot (-\mathbf{t}_- ds_- + \mathbf{T}_- dS_-) \tag{11}$$

The Griffith criterion, accounting for energy conservation, indicates that the elastic energy released is compensated by the energy expense of cracks propagation and delamination. For the case of a middle crack linked to the upper front, this is, $dE_r = \Gamma(dA_+ + dA_-) + G_c h(ds_+ + dS_+ + dS_-)$ wich leads to,

$$\begin{aligned}
&\left[(C_+(\Gamma_{S_+})\mathbf{n}_+ + D_+\mathbf{u}_+)\cdot\mathbf{T}_+ - (G_c h - \gamma e h)\right] dS_+ \\
&+ \left[(C_-(\Gamma_{S_-})\mathbf{n}_- + D_-\mathbf{u}_-)\cdot\mathbf{T}_- - (G_c h - \gamma e h)\right] dS_- \\
&\quad + \left[(C_+(\Gamma_{s_+})\mathbf{n}_+ - D_+\mathbf{u}_+)\cdot\mathbf{t}_+ ds_+\right] \\
&\quad + \left[(C_-(\Gamma_{s_-})\mathbf{n}_- - D_-\mathbf{u}_-)\cdot\mathbf{t}_- ds_-\right] \\
&\quad - \left[(G_c h - \gamma e h) ds_+ + \gamma e h ds_-\right] = 0
\end{aligned} \tag{12}$$

where, $C_\pm = (e - \Gamma_\pm) l_\pm / 2$ and $D_\pm = e f'(l_\pm) = e(\beta h - 2\alpha l_\pm)$. For simplicity used the notation that shows before where $\mathbf{F}_\pm = (C_\pm \mathbf{n}_\pm + D_\pm \mathbf{u}_\pm)$ and $\mathbf{f}_\pm = (C_\pm \mathbf{n}_\pm - D_\pm \mathbf{u}_\pm)$. In order to derive the propagation equations for cracks and follower front, we apply independent progression for each variable. This is,

$$\mathbf{F}_+ . \mathbf{T}_+ + \gamma e h = G_c h \tag{13}$$
$$\mathbf{F}_- . \mathbf{T}_- + \gamma e h = G_c h \tag{14}$$
$$\mathbf{f}_- . \mathbf{t}_- - \gamma e h = 0 \tag{15}$$
$$\mathbf{f}_+ . \mathbf{t}_+ + \gamma e h = G_c h, \tag{16}$$

which were presented in the main text.

II. SYMMETRIC 3 CRACKS

In the case of symmetric propagation of three cracks (as in the inset of main figure 2), we may directly take equation (12) with $ds_\pm = ds$ and $\mathbf{t}_\pm = \mathbf{t}$, and find the equivalent of (13-15) in this symmetric case:

$$(\mathbf{f}_+ + \mathbf{f}_-) . \mathbf{t} = G_c h \tag{17}$$
$$\mathbf{F}_\pm . \mathbf{t} + \gamma e h = G_c h \tag{18}$$

where $\mathbf{F}_\pm$ must also be aligned with the direction of propagation $\mathbf{t} = \cos\theta \mathbf{n} - \sin\theta \mathbf{u}$, where θ is the angle between the delamination front $\mathbf{n}$ and the direction of propagation $\mathbf{t}$. Together with this information, equation (18) can be replaced by $|\mathbf{F}_\pm| = G_c h - \gamma e h$ together with

$$\sin\theta = -\frac{e(2\alpha l_T - \beta h)}{(G_c - \gamma e)h} \qquad \cos\theta = \frac{(e - \Gamma) l_T}{2(G_c - \gamma e)h} \tag{19}$$

where l_T is the length of the debonding fronts. Equation (17) for the central crack writes $(e - \Gamma_s) l_T \cos\theta + 2e(\beta h - 2\alpha l_T)\sin\theta = G_c$, which, using (19) leads to

$$\cos 2\theta = \frac{G_c}{2(G_c - \gamma e)} \tag{20}$$

Finally, using this value for θ, equations (19) lead to

$$l_T = \frac{\beta h}{2\alpha} + \frac{G_c h}{2\sqrt{2}\alpha e}\sqrt{\left(\frac{\gamma e}{G_c} - 1\right)\left(\frac{\gamma e}{G_c} - \frac{1}{2}\right)} \tag{21}$$

$$\Gamma = e - \frac{\sqrt{2} G_c h}{l_T}\sqrt{\left(\frac{\gamma e}{G_c} - 1\right)\left(\frac{\gamma e}{G_c} - \frac{3}{2}\right)} \tag{22}$$

III. EXPERIMENTAL CHARACTERIZATION OF THE ADHESION ENERGY

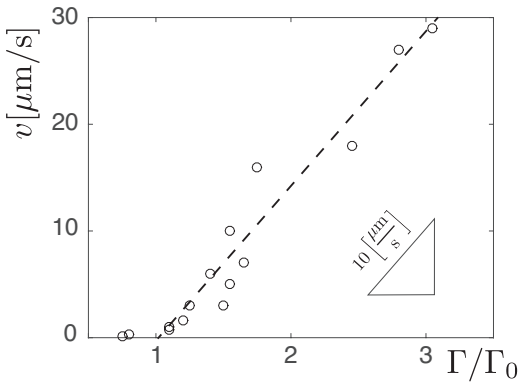

FIG. S3. Velocity of a delamination front v as a function of the adhesion energy Γ normalized by the adhesion energy at vanishing speed Γ_0. The dashed line is a linear fit $v = \eta(\Gamma/\Gamma_0 - 1)$ of the experimental data.

In Fig. S3, we plot the variation of the velocity of the delamination front v as a function of the adhesion energy Γ normalized by the adhesion energy at vanishing speed Γ_0. The adhesion energy is measured by monitoring the shape of a delamination front around a fixed straight crack as proposed by Jensen et al. [4]. The aspect ratio of the front depends on the ratio of the residual stress σ_0 with a critical stress σ_c, on the Poisson ratio of the film and on only moderately on a parameter accounting for mode 3 contribution at the tips of the straight

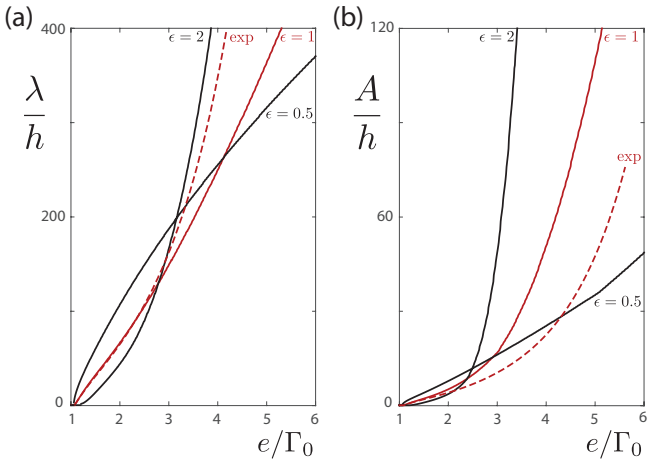

FIG. S4. Dimensionless wavelength λ/h (a) and dimensionless amplitude A/h (b) of oscillation vs. e/Γ_0. Solid lines represents power velocity laws $\eta(\Gamma/\Gamma_0 - 1)^\epsilon$, dashed red lines are obtained for an exponential law $v_0\left[1 - e^{-\varphi(\Gamma/\Gamma_0 - 1)}\right]$ where $v_0 = 4.5\,\mu$m/s and $\varphi = 1$. All curves are traced with $\eta = 4.5\,\mu$m/s and $\gamma e/G_c$ =0.49.

crack [3]. The adhesion energy $\Gamma(v)$ can thus be inferred from the shape of the front [3].

A simple linear description of the adhesion energy with the velocity, $\Gamma(v) = \Gamma_0(1 + v/\eta)$, is coherent with the experimental measurements in the experimental range. This description is also compatible with independent experimental measurements in other similar systems [5, 6]. To show the generality of the instability process, we next test the robustness of the oscillations to other kinetic lax (i.e. the dependence of the adhesion energy with velocity) and the effect of the kinetic law on the selection of the geometry of the oscillations.

IV. EFFECT OF KINETIC LAW ON WAVELENGTH AND AMPLITUDE OF OSCILLATIONS

In order to investigate the influence of the delamination speed on the oscillation features, we compute numerically the wavelength and amplitude and oscillations for different kinetic laws, namely, power laws: $v = \eta(\Gamma/\Gamma_0 - 1)^\epsilon$, with $\epsilon = 0.5$, 1 and 2, and an exponential law based on experimental observations on similar systems [5]: $v = v_0(1 - e^{-\varphi(\Gamma/\Gamma_0 - 1)})$, where v_0 is a limiting speed and φ a decay coefficient of order 1. Figure S4 compares wavelength and amplitude of oscillations for power laws, with $\eta = 4.5\,\mu$m/s and for an exponential law with $v_0 = 4.5\,\mu$m/s and $\varphi = 1$, such that in the limit of $\varphi(\Gamma/\Gamma_0 - 1) << 1$, the exponential tends to the linear law with the same value of $\eta = 4.5\,\mu$m/s. In all cases, oscillatory cracks are observed and the instability process appears for all the kinetic laws considered, albeit with different pattern geometry.

[1] J. W. Hutchinson and Z. Suo, Adv. Appl. Mech. **29**, 63 (1992).
[2] J. Marthelot, B. Roman, J. Bico, J. Teisseire, D. Dalmas, and F. Melo, Phys. Rev. Lett. **113**, 085502 (2014).
[3] J. Marthelot, J. Bico, F. Melo, and B. Roman, J. Mech. Phys. Solids **84**, 214 (2015).
[4] H. M. Jensen, J. W. Hutchinson, and K.-S. Kim, Int. J. Solid Structures **26**, 1099 (1990).
[5] Y. Lin, T. Y. Tsui, and J. J. Vlassak, Acta Mater. **55**, 2455 (2007).
[6] Y. Lin, T. Y. Tsui, and J. J. Vlassak, J. Electrochem. Soc. **157**, G53 (2010)